SPECIAL
Spontaneous Imbalance
COLLECTION

Spontaneous Imbalance and Hybrid Vortex–Gravity Structures

M ICHAEL E. M C I NTYRE

Centre for Atmospheric Science at the Department of Applied Mathematics and Theoretical Physics,
University of Cambridge, Cambridge, United Kingdom

ABSTRACT

After reviewing the background, this article discusses the recently discovered examples of hybrid propagating structures consisting of vortex dipoles and comoving gravity waves undergoing wave capture. It is shown how these examples fall outside the scope of the Lighthill theory of spontaneous imbalance and, concomitantly, outside the scope of shallow-water dynamics. Besides the fact that going from shallow-water to continuous stratification allows disparate vertical scales—small for inertia–gravity waves and large for vortical motion—the key points are 1) that by contrast with cases covered by the Lighthill theory, the wave source feels a substantial radiation reaction when Rossby numbers $R \gtrsim 1$, so that the source cannot be prescribed in advance; 2) that examples of this sort may supply exceptions to the general rule that spontaneous imbalance is exponentially small in R; and 3) that unsteady vortical motion in continuous stratification can stay close to balance thanks to three quite separate mechanisms. These are as follows: first, the near-suppression, by the Lighthill mechanism, of large-scale imbalance (inertia–gravity waves of large horizontal scale), where ''large'' means large relative to a Rossby deformation length L_D characterizing the vortical motion; second, the flaccidity, and hence near-steadiness, of L_D-wide jets that meander and form loops, Gulf-Stream-like, on streamwise scales $\gg L_D$; and third, the dissipation of small-scale imbalance by wave capture leading to wave breaking, which is generically probable in an environment of random shear and straining. Shallow-water models include the first two mechanisms but exclude the third.

1. Introduction

Lighthill's celebrated paper of 1952[1] was the first to study spontaneous imbalance. It is relevant to some cases of spontaneous imbalance and not to others. Here I begin with a review of the Lighthill theory and its genesis, then go on to discuss some examples that violate its assumptions.

One such example is the hybrid vortex–gravity instability discovered by Miles (1957), the first of many such hybrid instabilities known today. Another is the example discovered by O'Sullivan and Dunkerton (1995, hereafter OSD95), in which spontaneous imbalance in a

nonlinear baroclinic-wave life cycle of type 1 (LC1; e.g., Thorncroft et al. 1993 and references therein) produces internal inertia–gravity waves having small scales close to the grid scale of the numerical model. The small scales seem to put OSD95's example at an opposite extreme to those in which the Lighthill theory is relevant. The Lighthill theory describes scenarios in which unsteady vortical motion spontaneously emits inertia–gravity waves having horizontal scales large in comparison with the horizontal scales of the vortical motion. Thus, there was an understandable suspicion, at first, that gravity waves on scales close to the grid scale could, perhaps, be numerical artifacts.

However, with the growth of computer power it has become clear from very many subsequent studies that spontaneous imbalance of the kind found in OSD95 is a real fluid-dynamical phenomenon, not a numerical artifact. Conspicuously similar to OSD95 have been the examples recently discovered by Snyder et al. (2007, hereafter S07) and Viúdez (2006, 2007, 2008, hereafter respectively V06, V07, and V08), in which the vortical motions are, however, much simpler, consisting of

---

propagating vortex dipoles. In further contrast with the Lighthill theory, the gravity wave emission is revealed as a *steady,* mountain-wave-like process in the sense that the waves have zero phase speed in the comoving reference frame. Before that, Snyder et al. (1993) had studied gravity wave emission from a collapsed surface front held steady by numerical diffusivities—already showing the possibility of an essentially steady wave emission process—and Plougonven and Snyder (2005) had shown by careful analysis that the reason for the small scales in examples like OSD95 is not the wave emission process at all, but rather the subsequent refraction leading to ''wave capture.'' This turns out to be true of the dipole examples as well.

Wave capture explains the tendency for the gravity wave scales to approach the grid scale in the OSD95 and dipole cases. Wave capture is the counterpart of critical-layer absorption that results not from vertical shear alone but from the straining of wave crests by large-scale horizontal deformation fields, modified by vertical shear (Jones 1969; Badulin and Shrira 1993). A comprehensive review may be found in Bühler and McIntyre (2005). The horizontal straining shrinks the wavelength exponentially fast, rather than algebraically. The wave packet behavior becomes passive-tracer-like as the group velocity goes to zero. Mathematically, the flow fields tend toward a singular limit. More physically relevant is that the linearized wave theory predicts its own breakdown in a manner suggesting the onset of wave breaking in reality.

The new dipole examples have turned out to be of key importance in that they have allowed the wave source region and mechanism to be identified unequivocally, as summarized in section 6 below. The horizontal and vertical scales of the source region are broadly comparable to the scales of the dipole itself and are much larger than the scales of the most conspicuous gravity waves, which are those undergoing capture at some remove from the source. However, for order-unity Rossby and Richardson numbers there is no scale separation within the source region. The wave source is therefore strongly influenced by the radiation reaction exerted on the source region by the waves. In the dipole examples this radiation reaction has a recognizable fingerprint, in that it destroys the fore–aft symmetry of what would otherwise be a balanced omega or vertical-velocity field. The fore–aft asymmetry becomes conspicuous—completely reshaping the omega field—as soon as Rossby and Richardson numbers attain order-unity values. In terms of the mountain wave analogy, the radiation reaction drastically reshapes the mountain. One cannot specify the mountain shape in advance. By contrast, the main point of the Lighthill theory is that, when the theory applies, the radiation reaction is so weak that one can, in principle, prescribe the wave source in advance.

There is a final twist in the tail of this tale. There is a sense in which consistent high-order potential vorticity (PV) inversion operators (hyperbalance inversion operators) appear capable of delivering not only the vortical motion but also the comoving gravity waves, as explained in the concluding remarks below. This makes a peculiarly unexpected connection with the generalized, Bayesian PV inversion operators proposed, for quite different reasons, by Hakim (2008).

This article is dedicated to my former student Rupert Ford, whose meteoric career was tragically cut short on 30 March 2001 (McIntyre 2001, 2008), and to my former colleague Sir James Lighthill who died on 17 July 1998, in typically magnificent style, on one of his ''adventure swims'' around the island of Sark. Both were extraordinary thinkers who made far-reaching contributions to our subject, and both were persons of exemplary warmth, generosity, and scientific integrity.

2. Lighthill's theory of acoustic imbalance

While still a terrifyingly bright young man—fresh from wartime aerodynamics after his journey through pure mathematics with schoolmate Freeman Dyson—James Lighthill (1952) singlehandedly put his finger on a key aspect of the phenomenon of spontaneous imbalance.

Addressing the problem of noise emitted by jet aircraft, Lighthill studied the simplest thought experiment in which the phenomenon arises. For unstratified, nonrotating, compressible flow in an unbounded domain with no gravity or other external force, he asked how a freely evolving vortical flow occupying some finite region might emit sound waves, even when the Mach number $M = U/c_s \ll 1$. Here, U is a typical flow speed and c_s is the sound speed. By combining simple mathematics with a careful and powerful heuristic argument based on physical insight, Lighthill showed that practically any unsteady vortical flow will spontaneously emit sound for any value of M, however small. He also showed that through destructive interference the sound emission is surprisingly weak when $M \ll 1$, far weaker than one would estimate from naive order-of-magnitude analyses. The ideas are well known and are reviewed, for instance, in Ford et al. (2000, section 2). From an atmosphere–ocean dynamics perspective, the emission of sound may be viewed as the simplest possible example of spontaneous imbalance. In Lighthill's original problem, the balance is elastostatic. Sound waves represent the only possible kind of imbalance.

If the spontaneous emission of sound can be neglected—that is, if one can neglect the imbalance—then one can

describe the dynamics in the classical way as a purely vortical flow. What does that mean? The crucial feature is that one can invert the vorticity field at each instant to obtain the velocity, pressure, and density fields.

In an unbounded domain, one can do this via the Biot–Savart integral [e.g., Batchelor 1967, Eq. (2.4.11)] or refinements thereof. One can equally well invert what might be called the acoustic PV. This is the vorticity divided by the mass density. It has the simplest evolution equation and visualizability [e.g., Batchelor 1967, Eq. (5.3.6)]. Invertibility means that there is a purely diagnostic functional relation—nonlocal, of course—between the vorticity or PV field and everything else. Knowledge of the vorticity or PV field at one instant implies knowledge of everything else at that instant. One can therefore use the standard language of aerodynamics and speak of the velocity field ''induced'' at each instant by a given vorticity field (e.g., Lighthill 1963). Thinking thus in terms of vorticity or PV inversion makes explicit the most basic peculiarity of vortex dynamics—the point missed when only local balances of terms are considered—the apparent action at a distance whereby a vortex contributes instantaneously to the motion of other vortices.

Of course such action or influence cannot really travel faster than sound. But Lighthill's arguments showed, in effect, that using balance and invertibility to describe the vortex dynamics, as if one did have instantaneous action at a distance, can be far more accurate than naive order-of-magnitude analysis would predict. And, as Lighthill was careful to point out, that is the very reason why his ideas make sense. The prediction of destructive interference and therefore weak sound emission depends on being able to suppose that the vortical flow can be regarded as known, in principle, independently of the sound emission:

> All the evidence of experiment, and of the theory to be developed below, is that the sound produced is so weak relative to the motions producing it that no significant back-reaction can be expected ... (Lighthill 1952)

This means that one can in principle compute the vortical flow evolution to high accuracy—and the weaker the spontaneous emission, the higher the accuracy—then afterward compute the emission with the nonlinear terms treated as known source terms in a wave equation. The destructive interference arises from the long wavelength λ of the sound emitted, relative to the scales of the vortical motion, and the special form of the source terms for all cases of vortex motion. Each term takes the form of a second spatial derivative [Lighthill 1952, Eq. (4c); Ford et al. 2000, Eq. (2)]. Thus, the whole picture is self-consistent—the more so, the weaker the emission (Ford et al. 2002).

3. Shallow-water rotating flow

The ideas of balance, imbalance, and PV inversion carry over at once to shallow water dynamics with only trivial changes of wording. Sound waves are replaced by gravity waves. The Mach number $M = U/c_s \ll 1$ is replaced by the Froude number, in its standard sense $F = U/c \ll 1$, where c is the gravity wave speed. The acoustic PV is replaced by the Rossby PV, absolute vorticity divided by layer depth (Rossby 1936).[2]

It is well known that the shallow-water equations are identical to the two-dimensional equations for a perfect gas with $\gamma = 2$. Here, γ is the ratio of specific heats, whose numerical value is an unimportant detail. So Lighthill's ideas carry over without modification as long as there are no Coriolis terms. For two-dimensional flow, the weakening of spontaneous imbalance and spontaneous gravity wave emission as F diminishes can be expressed by saying that if c is held constant while U is diminished, then the gravity wave power radiated goes as U^7. The corresponding *dimensionless* measure of imbalance in two dimensions is F^4 (Ford et al. 2000).

If Coriolis terms are introduced, then Lighthill's ideas still carry over qualitatively (Ford et al. 2000, 2002). Pure gravity waves are replaced by inertia–gravity waves. The problem is no longer identical to Lighthill's

---

[2] A reviewer has insisted that the PV concept dates from well before 1936. That is arguably the case provided that one uses the Lagrangian description of fluid dynamics. Then the material invariance of PV for ideal fluid flow is a straightforward corollary of nineteenth-century vortex dynamical theory. Most simply, the Rossby–Ertel PV is proportional to the absolute Kelvin circulation around an infinitesimally small closed material contour C lying on a stratification surface, isentropic or isopycnal—or on the free surface of a shallow-water system—divided by the mass of the infinitesimal material fluid element whose perimeter is C. For continuous stratification this element is bounded above and below by neighboring stratification surfaces [for more detail, see McIntyre (2003)]. Thus, PV invariance follows almost trivially from mass conservation and Kelvin's circulation theorem. By using the full machinery of the Lagrangian description, one may also relate the PV to a quantity from nineteenth-century theory called ''Beltrami's material vorticity'' (Viúdez 2001). This is a way of describing the three-dimensional vorticity field mapped into Lagrangian label space. The mapping is defined as a kinematically possible fluid flow with the vortex lines and stratification surfaces frozen into the fluid. Of course the usefulness of the PV concept as first published by Rossby, both for shallow water (Rossby 1936) and for multilayer and continuous stratification (Rossby 1940), lies in being able to avoid the Lagrangian description. This is useful because, for one thing, PV inversion is quintessentially an Eulerian or field-theoretic procedure. We may note that 1936 is also the year in which Lighthill began his high-school mathematical journey with Dyson at the age of 12, and 1940 the year in which they were both prevented, by their youth, from going on to Cambridge despite having won scholarships.

because, for one thing, the far field into which inertia–gravity waves are radiated is now at rest in the rotating frame rather than in an inertial frame. Furthermore, there are now two small parameters. The vortical motion is characterized by a Rossby number R as well as by a Froude number F, and there are a variety of asymptotic limits corresponding to R or F, or both, being small in one sense or another. The full Lighthill picture has been shown by detailed asymptotic analysis to apply in the limit where $F \to 0$ faster than R, that is, with $F \ll R$ (Ford et al. 2000), in which case the dimensionless spontaneous imbalance is still $O(F^4)$ as $F \to 0$. However, in complementary cases where $R \to 0$ with $F \gtrsim R$, the spontaneous imbalance tends to become exponentially small in R (Ford 1994; Ford et al. 2002; Vanneste and Yavneh 2004; Wirosoetisno 2004; Ólafsdóttir et al. 2008; Temam and Wirosoetisno 2007; R. Temam and D. Wirosoetisno 2008, manuscript submitted to SIAM *J. Math. Anal.*, hereafter TW).[3]

Ford et al. (2002) argued that this exponential smallness—associated with vortical-flow unsteadiness, with smooth time dependence implying an exponentially decaying spectral tail—makes Lighthill's ideas still more powerful. Not only is the back-reaction still weaker, but on top of that, in some cases at least, the destructive–interference aspect remains significant. The inertia–gravity wave frequencies emitted tend to be so close to the inertial frequency f that horizontal wavelengths $\lambda \gg L_D$, where L_D is the Rossby deformation length. Vortical flows often have horizontal scales $\sim L_D$ not only in the shallow-water system but also in stratified cases in which there is a dominant vertical scale.[4] The recent work of Ólafsdóttir et al. (2008) confirms the $\lambda \gg L_D$ behavior in a clear-cut stratified case in which a weak ellipsoidal vortex of horizontal dimension L_D is sheared horizontally by a background flow. In that case, λ scales as $R^{-1}L_D$ as $R \to 0$. Most importantly, the weakness of the back-reaction continues to mean that PV inversion can be accurate—indeed, yet more accu-

rate than before—with exponentially rather than algebraically small error.

4. The slow quasimanifold

Lighthill's ideas, and their extension to rotating systems, remain important also in their complementary aspect. The wave equation with an unsteady wave-source term shows that spontaneous imbalance, weak though it may be, must be generically nonzero if we discount the unlikely event that destructive interference is perfect. Robustly, therefore, albeit heuristically, Lighthill's arguments are enough to show that there can be no such thing as an invariant slow manifold of the primitive equations, in the strict sense of Leith and Lorenz. This aspect was emphasized and carefully discussed by Ford et al. (2000, 2002). The idea of a slow manifold—a sharply defined hypersurface within phase space, with zero thickness—must be replaced by the idea of a fuzzy "slow quasimanifold," a chaotic layer or stochastic layer of finite thickness, of the generic sort familiar from studies of low-order dynamical systems, such as the perturbed simple pendulum.

As did Rupert Ford, I prefer to avoid self-contradictory terms such as "fuzzy manifold," "hairy bald head," "asymmetric symmetric baroclinic instability," "ageostrophic geostrophic adjustment," and so on, despite the ubiquity of such terms in human language (e.g., McIntyre 1997)—hence the term "slow quasimanifold" advocated in Ford et al. (2000). Accuracy of balance and inversion means only that the layer is thin, not that it is actually a manifold.

Historically, understanding could well have been impeded, as often happens, by the persistence of self-contradictory language together with the Humpty Dumpty credo that words are unimportant. The "fuzzy slow manifold"—the "hairy bald head" of atmosphere–ocean dynamics—was recognized independently, long ago, by some researchers at least (Errico 1982; Warn 1997).[5] Back then it seems that Errico and Warn had no knowledge of Lighthill's original work. However, Errico's sections 9 and 10 take us very close to Lighthill's ideas, including the insight that the inertia–gravity or fast modes of the standard normal-mode description respond directly to high frequencies existing within the quasi-geostrophic solution, i.e., to the "tail" of the geostrophic power spectrum (Errico 1982, p. 585b).

---

[3] In case the reader wishes to consult this manuscript, it is available at the entry numbered 0808.2878 in the well-known on-line database at arXiv.

[4] This is especially clear for continuously stratified cases in which the buoyancy frequency N is not too strongly variable. Theory and laboratory experiment with $N \sim$ constant indicate that not only the velocity and buoyancy fields but also the vortex cores themselves, the PV anomalies, tend to have horizontal-to-vertical aspect ratios of the order of Prandtl's ratio N/f. Other aspect ratios are usually unstable (e.g., Miyazaki and Fukumoto 1992; Dritschel and de la Torre Juárez 1996; Billant and Chomaz 2000). In other words, the horizontal scale $\sim L_D$ when L_D is defined as the vertical scale times N/f.

---

[5] The correct date for Warn's pioneering contribution is 1983. However, bureaucracy prevents me from acknowledging this in the list of references. Warn's contribution was rejected for publication in 1983, being perhaps too far ahead of its time.

Errico's section 9 tests the idea that one can first describe the vortical motion by itself and then afterward treat it as a known source for inertia–gravity waves, essentially as in Lighthill. Warn's paper was the first to point out, explicitly, that the evidence from Errico's work argued against the existence of a slow manifold.

Just how thin the slow quasimanifold can be in shallow-water flows, how *nearly* manifold-like, with order-unity values of F and R, well outside the parameter regimes to which Lighthill's ideas are manifestly applicable, remains astonishing and still poses a challenge to our understanding. High-order shallow-water balanced models based on advecting the exact Rossby PV were first shown by Norton (1988) to maintain an uncanny accuracy over several eddy turnaround times, as judged by their ability to track primitive equation evolution even for order-unity values of F and R; see also McIntyre and Norton (1990, 2000, hereafter MN00), and Mohebalhojeh and McIntyre (2007b). This behavior was a total surprise when it was first discovered. However, the uncanny accuracy—and, by implication, the weakness of spontaneous imbalance in these particular flows despite order-unity F and R—can with hindsight be related to the flaccidity and slow evolution of jets meandering Gulf-Stream-like, or river-like, on scales much larger than the Rossby deformation length L_D (e.g., Nycander et al. 1993 and references therein; McIntyre 2008 and references therein). The relative thinness $\sim L_D$ and near-steadiness of such jets helps to keep their Lagrangian time scales considerably longer than inertia-wave time scales f^{-1}, even for order-unity values of the Rossby number R based on jet width L_D. This is so far outside the scope of Lighthill theory that the jet flaccidity, or fluviality, characteristic of the regime $R \sim F$ and apparently persisting out to $R \sim F \sim 1$, is probably best considered as a separate, second mechanism for keeping flows close to balance.

5. Some classic hybrid vortex–gravity structures

It is crucial to Lighthill's picture that the vortical motion be unsteady. If only for that reason, the propagating dipole vortex–gravity structures described in S07 and in V06, V07, and V08 must fall entirely outside any such picture. The propagation of those structures is very close to being steady. Before discussing them we may remark that other such hybrid structures have long been known in which, however, the vortical part itself takes the form of a wave—a Rossby wave in the natural, generalized sense of the term, propagating on a gradient of vorticity or PV (e.g., Miles 1957 and

very many others).[6] Here the typical scenario is an exponentially growing instability consisting of a counter-propagating, phase-locked pair of waves, one being a Rossby and the other a gravity wave. However, in some cases there are also neutrally stable, steadily propagating modes at certain wavelengths. Because of the steadiness or near-steadiness, it is again clear that we have examples of spontaneous imbalance that fall outside any Lighthill-type scenario.

Lighthill himself cautioned that there would be exceptions to his theory. Here is how he continues the passage quoted in section 2 above:

> . . . no significant back-reaction can be expected unless there is . . . a resonator present to amplify the sound

or, in the present context, the gravity wave. That is, the self-consistency of Lighthill's picture depends on excluding resonance phenomena. The hybrid instabilities just mentioned can, of course, be recognized as resonance phenomena. The Miles (1957) instability is a clear-cut example. The gravity wave is a surface gravity wave on water, and the Rossby wave propagates on a vertical vorticity gradient in the air above. Once they are phase-locked together, each wave resonantly excites the other. So if we say that the Rossby wave excites the gravity wave, then we must admit that, equally, the gravity wave exerts a significant back-reaction on the Rossby wave.

6. Vortex dipoles in continuous stratification

The dipole examples of S07 and of V06, V07, and V08—and by implication the OSD95 example and its successors—belong in yet another category. Continuous stable stratification is an essential factor. The spontaneous imbalance in these examples is quite different from that in classical Lighthill-type scenarios and quite different, also, from that in the hybrid instabilities and their neutral modes.

Rather than an equal partnership between the vortical and gravity wave parts, each of which resonantly excites the other, we have what looks at first sight like a master–slave relation—"slave" in the general sense and not the slow-manifold sense—and, to that extent, something more like a Lighthill scenario. There is no resonance

---

[6] The idea of explaining shear instabilities in terms of phase-locked counterpropagating waves has a long history, going back at least as far as Taylor (1931) and Lighthill (1963, p. 93). Taylor's classic paper is reproduced on pp. 219–239 of *The Scientific Papers of Sir Geoffrey Ingram Taylor*, vol. II, ed. G. K. Batchelor, Cambridge University Press, (1960). The idea has been greatly developed in recent years; see, for example, Ford (1994), Methven et al. (2005), and references therein.
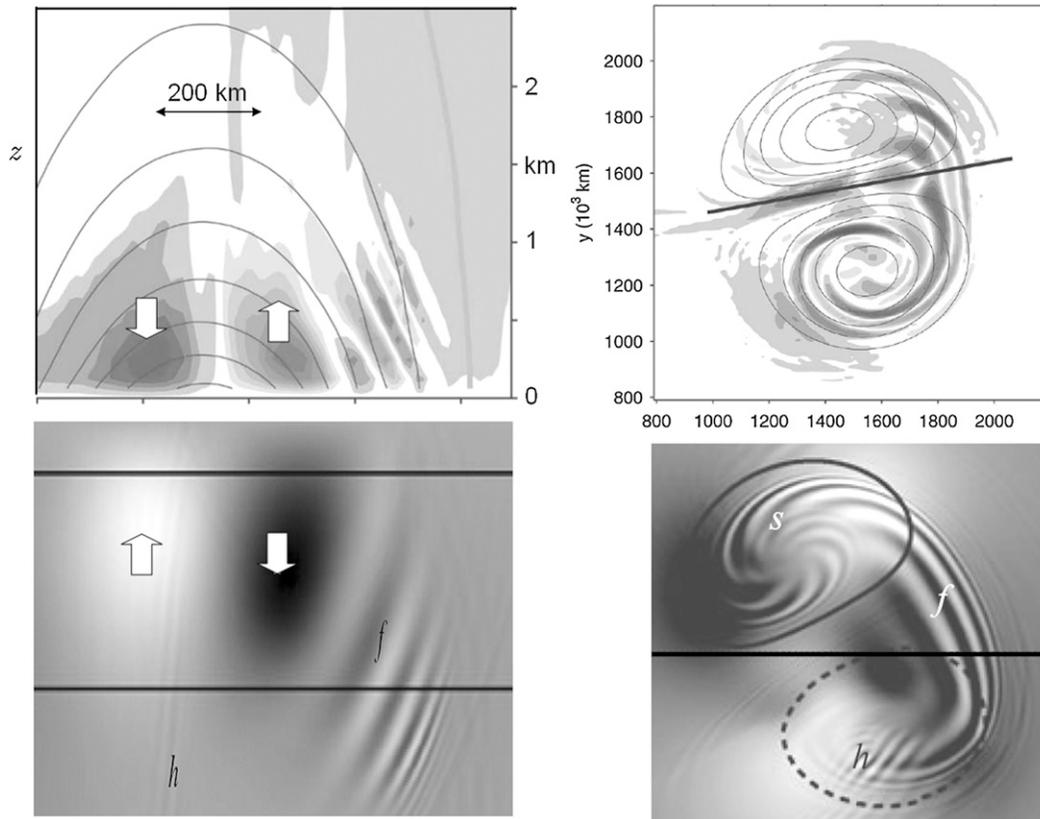
FIG. 1. Rightward-propagating 3D vortex dipoles shown by vertical and horizontal sections representing the two best-resolved cases in S07 (top panels) and in V06, V07, and V08 (from V07, bottom panels). The vertical sections on the left are taken along the heavy straight lines seen in the horizontal sections on the right. The gray shading in each panel shows the omega or vertical velocity field, which oscillates around zero with signs indicated by the white arrows. The vertical section at bottom left shows the bottom half, $z < 0$, of the dipole described in V07. The heavy horizontal lines mark depths z with nominal values -0.21, -0.9 in the dimensionless units used in V07. The horizontal section at bottom right is at $z = -0.9$, and at top right is at $z = 0.25$ km. The vertical section at bottom left has been expanded vertically so as to agree with the coordinate aspect ratio of the section at top left after scaling by Prandtl's ratio N/f, whose value at top left is 100 ($= 200$ km/2 km). Further detail can be seen in S07's Figs. 10 and 11 and in V07's Figs. 1–4 and 11–15. In V07's Fig. 2 the origin of coordinates needs correction: the horizontal midplane of the dipole is at $z = 0$. The top half of the dipole is never shown. The three-dimensional PV anomalies in V07's case occupy the vertical range $-1.2 \leq z \leq 1.2$ approximately. The nominal z values are Boussinesq isopycnal coordinate values defined in terms of the 512 stratification layers used in the numerical discretization, representing continuous stratification to good approximation. The computational domains are larger than shown and are respectively a doubly periodic domain with a sponge lid in S07 and a triply periodic domain in V07. The thin contours at top left mark horizontal rightward flow speeds $|\mathbf{v}| = 1, 2, 3,\ldots, 7$ m s^{-1} in the comoving frame of reference. The faint thick contour marks the separatrix or $|\mathbf{v}| = 0$ surface. The thin contours in the horizontal section at top right give the surface potential temperature field, the Bretherton PV delta function whose inversion dominates S07's dipole structure.

here, as shown shortly. However, on closer examination we shall see that it is not a case of master and slave either. Appearances are deceptive in this regard.

Figure 1 summarizes the two best-resolved examples, with vertical sections on the left and horizontal on the right. The top left panel, after S07's Fig. 9, shows the streamwise vertical midplane for a dipole structure induced mainly by a distribution of potential-temperature anomalies on a solid bottom bound-

ary $z = 0$. This is equivalent to a Bretherton PV delta function. The interior PV is isentropically uniform, to a first approximation. The faint thick contour on the right of the top left panel marks the separatrix or $|\mathbf{v}| = 0$ isotach in the comoving reference frame, where $|\mathbf{v}|$ is horizontal flow speed. The other contours are the isotachs for horizontal rightward flow speeds 1, 2, 3, . . . , 7 m s^{-1} in the comoving frame. The shading shows the omega or vertical velocity field (see caption). The most

conspicuous gravity waves are the nearly plane waves inside the separatrix. In the wave-capture limit, the wavelength tends to zero and the wave crests tilt toward the isotachs, as verified in finer detail in S07's Fig. 10.

The bottom left panel, after V07's Fig. 2, shows in grayscale the vertical velocity field in the bottom half of a different dipole flow. Here there are no solid boundaries. Instead of a PV delta function, there are continuously distributed PV anomalies occupying a substantial volume within the three-dimensional dipole structure. The vertical section is slightly skewed from the streamwise vertical midplane but shows a view that would be qualitatively similar to the streamwise vertical midplane view. The complete picture in the vertical midplane is therefore qualitatively like the bottom left panel together with its sign-reversed reflection in a horizontal mirror at $z = 0$, in other words, qualitatively like the two left-hand panels viewed together. Both the small-scale gravity waves and the central pattern of vertical velocities, marked by the white arrows, are similar in the two cases despite the very different PV distributions.

In the horizontal sections on the right (see caption), the shading again shows the vertical velocity field. In both cases the most conspicuous gravity waves are being advected cyclonically and anticyclonically around each half of the dipole, precisely as expected from a wave-capture scenario. The cyclonic–anticyclonic asymmetry is related to the fact that Rossby numbers R are not small. Indeed, R values are close to unity in a natural quantitative sense to be made precise in the next section.

Now the most conspicuous gravity waves are nearly plane waves in a locally valid approximation. They therefore have well-defined group velocities and their propagation can be well described by ray theory. In the vertical midplane the group velocities relative to the comoving frame, including the contribution from advection by the background flow, are directed across the wave crests and away from the central region. Apart from the diminishing wavelengths this is qualitatively the same as in classical mountain-wave problems with uniform flow and uniform buoyancy frequency N, satisfying a radiation condition at infinity.

We can therefore identify the source region unambiguously. It is the central region marked by the white arrows. We can also unambiguously deduce that the back-reflection required for resonant-cavity behavior is absent. Resonance has no role. In the standard ray-theoretical manner the propagation is accurately one-way, from the central source region toward the region of wave capture near the forward separatrix. The scale varies smoothly and continuously all the way from the half wavelength

indicated by the spacing of the white arrows down to the smallest scales approaching the separatrix.

As indicated schematically by the white arrows, the velocity field in the source region above $z = 0$ shows a simple pattern of excess descent behind the center of the dipole and excess ascent ahead, and vice versa below $z = 0$, where "excess" means additional to the larger-scale quadrupolar pattern of vertical motion characteristic of the quasigeostrophic limit. This point is most clearly brought out in S07's Fig. 11 (in the top row of color plots, not reproduced here). So on the streamwise vertical midplane of the dipole where the quasigeostrophic vertical motion vanishes, the streamlines and stratification surfaces bend toward the horizontal midplane or surface $z = 0$, at the center of which the rightward flow speed $|\mathbf{v}|$ in the comoving frame is close to maximal, as seen from the lowermost (7 m s^{-1}) contour at the top left in Fig. 1 above. The bending of the stratification surfaces toward $z = 0$, common to S07 and V07, is clearly a robust feature and is just what one would expect dynamically from the Bernoulli relation, together with hydrostatic balance and the crowding of streamlines around the central point on $z = 0$.

Now the Bernoulli and other inertial effects are not enough in themselves to cause substantial imbalance and wave emission. This point is clear from the known shallow-water examples, including those mentioned at the end of section 4. Bernoulli effects are strongly present in shallow-water motion at order-unity Froude and Rossby numbers F, R, for instance in the jet exit regions in MN00's Fig. 2a. However, in those examples they manifest themselves hardly at all as imbalance but rather, almost entirely, as nonlinear modifications to the balance condition and PV inversion operator. The same thing is seen in classic two-layer studies such as that of Van Tuyl and Young (1982), in which the comoving "gravity–inertia signal" is essentially the same nonlinear modification to balance, with negligible gravity wave emission. Bernoulli and other inertial effects are fully represented by nonlinear terms such as $\nabla \cdot (\mathbf{v} \cdot \nabla \mathbf{v})$ within all the most accurate balance and inversion operators. So a strong Bernoulli effect does not, of itself, necessarily imply substantial imbalance and a strong gravity wave source.

What most plainly distinguishes the present problem from the shallow-water and two-layer examples is the different wave dispersion relation for continuous stratification, which allows not only wave capture but also the freedom, in the wave field, to fit the central flow scales indicated by the half-wavelength spacing of the white arrows and the concomitant vertical scale with aspect ratio f/N. This permits wave emission with no spatial destructive interference as well as permitting the

waves to escape as though they satisfied a radiation condition, as already remarked.

Along with the order-unity R values this state of things implies, in turn, that there is a substantial back-reaction upon the central source region in the form of a radiation reaction, like the power drawn by an efficient radio antenna. In summary, 1) the order-unity importance of Bernoulli and other inertial effects and 2) the approximate spatial and temporal scale matching between the source and the emitted waves (temporal as well as spatial when $R \sim 1$) together imply that there is a radiation reaction on the central source region having a substantial, leading-order effect on the dynamics.

By itself, the Bernoulli effect in the streamwise midplane would produce a pattern of motion and stratification-surface distortion having fore–aft symmetry. This is the symmetry suggested by looking only at the white arrows and thin contours in Fig. 1. Indeed, such fore–aft symmetry is an exact property of balanced, purely vortical motion induced by PV anomalies with the same symmetry. It is related to the general time symmetry or "sign reversal property" discussed in Ford et al. (2000). So the fore–aft *asymmetry* in the vertical-motion fields actually found in the central region—conspicuous in the top right panel especially—must be a consequence of the radiation reaction. That conclusion is further supported by the top row of S07's Fig. 11, showing the vertical velocity field in five cases with R values 0.125, 0.5, 0.75, 1.0, and 1.5 times the value for Fig. 1 above. The first case shows almost perfect fore–aft symmetry and the others increasing fore–aft asymmetry, very strong in the last case.

This says, then, that when $R \gtrsim 1$ the wave emission is not an affair of master and slave. It is an affair of bootstrapping. That is, it depends on an intimate, two-way interplay between the inertial effects in the source region and the radiation reaction on that region, introducing a local arrow of time. The source emits the radiation, but the radiation reaction reshapes the source. It is as if one had a mountain-wave problem in which the mountain were elastic and substantially changed its shape in response to the surface-pressure field, in turn creating a large change in the vertical velocity field.

So we have here something that is about as far from a Lighthill scenario as it is possible to imagine. With the source strength so intimately dependent on the radiation reaction, the source strength cannot be considered to be known in advance. This insight is, of course, consistent with the standard remark that when $R \gtrsim 1$—see next section—one should not expect to be able to distinguish balance from imbalance (i.e., to distin-guish vortical motion from gravity wave motion) even in principle. The distinction becomes meaningless and the slow quasimanifold can no longer be regarded as thin in any sense. No mathematical device, no manipulation of the equations, however ingenious, can ever hope to produce a unique and clear-cut separation between balance and imbalance within such a source region. Arguably, a tendency to forget this fact has impeded understanding in past decades.

Further support for the picture just sketched comes from the work of V07 and V08. It was found there that even the iterative ramping procedure of Viúdez and Dritschel (2004) called "optimal PV balance"—perhaps the closest to an objective balancing procedure one is ever likely to get—failed to disentangle the flow within the central source region into balanced and imbalanced parts. (See the discussion on p. 364 of V07, noting incidentally that "upper" means slightly *below* the horizontal midplane $z = 0$.) In section 8 below we remark that a corresponding ambiguity shows up in the equations defining high-order balance and PV inversion operators.

7. The dependence on R

Let us look more closely at the role of the Rossby number R and the most natural way to define R in this problem. To get temporal as well as spatial scale matching in the central source region—an efficient radio antenna, so to speak—the particle travel time through a half wavelength of the pattern (say, τ_h) must satisfy $\tau_h \lesssim \pi / f$. That is, the travel time needs to be about half an inertial period or less. So it is natural to define R for this purpose in the standard Lagrangian sense (e.g., Hoskins 1975; Koch and Dorian 1988; Zülicke and Peters 2006, 2008 and references therein), as

$$R = R_{\mathrm{Lagr}} = \frac{\pi}{\tau_h f} \qquad (1)$$

and to anticipate that $R_{\mathrm{Lagr}} \gtrsim 1$ should characterize efficient radiation and a substantial radiation reaction on the central region not only qualitatively but also quantitatively to moderate accuracy.

From the spacing of the white arrows in S07's case at top left in Fig. 1 we see that the horizontal half wavelength there is close to 250 km. The particle velocity through the lowest part of the central region, between the bottom two contours, is around 6 m s^{-1}. If we take $\tau_h = 250 \times 10^3/6 = 4.2 \times 10^4$ s then, with $f = 1.0 \times 10^{-4}$ s^{-1} (S07, p. 4419a), we have $R_{\mathrm{Lagr}} = \pi/(\tau_h f) = \pi/4.2 = 0.75$. The two cases described in V07 and V08

have $R_{\mathrm{Lagr}} = 0.44$ and 1.1. The value $R_{\mathrm{Lagr}} = 1.1$ applies to V07's case reproduced in the lower half of Fig. 1 above.[7]

In S07 the case with the largest R_{Lagr} value (not reproduced here) has a value 1.5 times greater than for the case in Fig. 1 above. In the former case, showing very strong fore–aft asymmetry in the vertical velocity field (S07 Fig. 11, top right), we have $R_{\mathrm{Lagr}} = 0.75 \times 1.5$, just over 1.1.

We remark finally that some dipole examples of this sort may violate the usual rule that the strength of spontaneous imbalance diminishes exponentially as $R \to 0$. The reasons are as follows.

As $R \to 0$, particle travel times across the central region increase relative to π/f. Then quasi-steady, mountain-wave-like gravity wave emission has to rely on the diminishing spatial scales in the velocity and buoyancy fields that then correspond to intrinsic wave frequencies $\gtrsim f$. So the amplitude of wave emission will depend on a spatial projection integral whose integrand consists of a rapidly oscillating factor, representing the diminishing wave scales, multiplied by a slowly varying factor coming from the velocity and buoyancy fields of the vortex dipole. Thus, as R diminishes from order-unity values toward zero, destructive interference re-enters the problem, wave emission weakens, and to that extent a Lighthill-type treatment becomes appropriate again despite the motion being quasi-steady, and despite the scale

disparity being in the opposite sense, with gravity wave scales small relative to vortex scales.

The projection integral will diminish with R in a manner depending on the smoothness of the dipole's velocity field. With a completely smooth velocity field, perhaps smoothed by artificial viscosity, the integral, over the whole spatial domain, if infinite or periodic, may be expected to diminish exponentially. Indeed, such heuristics are consistent with a rigorous upper bound $O[\exp(-\mathrm{const.}\, R^{-1/4})]$ on spontaneous imbalance, recently established by TW on the assumption of diffusive flow (for buoyancy as well as momentum), together with compatible smoothness conditions (Gevrey regularity) and triply periodic boundary conditions as in V06, V07, and V08.

However, with nondiffusive, ideal-fluid flow and a velocity field that is less smooth (such as would be expected, for instance, with isentropic distributions of PV that have jump discontinuities), the projection integral might instead diminish algebraically with R. Here, the R dependence would be that of a set of ideal-fluid cases computed over a finite time interval before the onset of wave breaking via wave capture.

This speculation is based on the idea that the smoothness of the actual velocity and mass fields should be related to the smoothness of the fields produced by a PV inversion operator. Such operators are well known to be nonlocal smoothing operators but are, of course, incapable of producing velocity and mass fields that are infinitely smooth at a PV discontinuity. The projection integral expresses the nonlocal aspects of the wave emission dynamics and so might be expected to depend on the dipole's global fields and not just on, for instance, the shapes of particle trajectories, which in a steady flow must follow PV contours and may well be smoother than the velocity field itself. Taking these ideas further would be a severe mathematical challenge.

---

[7] For that case, R_{Lagr} is estimated at the nominal depth $z = -0.21$ in V07's dimensionless units, corresponding to the upper heavy line in the bottom left panel of Fig. 1 above. The half wavelength was measured from V07's Fig. 1a (not reproduced here), whose dimensionless length and width are both 20π units. The half wavelength is about 12 units. V07's Fig. 11a shows horizontal velocity vectors and isopleths at the same nominal depth, $z = -0.21$, in a plot whose dimensionless length and width are 45.5 units. From this information it can be determined that the flow through the central half wavelength is accurately along the streamwise midplane and lies mostly within the $|\mathbf{v}| = 2.5$ isopleth, the innermost isopleth surrounding a central maximum $|\mathbf{v}|$ value of 3.0 units. To go into the comoving frame, one must subtract ~ 0.2 units, so that on the streamwise midplane the values 2.5 and 3 become roughly 2.3 and 2.8 units. Taking the half-wavelength particle travel time as $\tau_h = 12/2.6$ units, and noting from V07 (p. 362) that $\pi/f = 5$ units exactly, we get $R_{\mathrm{Lagr}} = 5/(12/2.6) = 1.1$. The case with $R_{\mathrm{Lagr}} = 0.44$ is most thoroughly described in V08, where Fig. 16 presents particle travel-time isochrones. The travel time through a quarter-wavelength in the central source region, between the center of the region and the first vertical velocity extremum, can be read off from the figure as about 1.6 isochrone intervals. This can be seen to be $1.6\sqrt{2}/4$ in units of the inertia period, after correcting a typographical error in the caption, where $\sqrt{2}/2$ should be $\sqrt{2}/4$. So the time through a central *half* wavelength is $6.4\sqrt{2}/4$ *half* inertia periods, making $R_{\mathrm{Lagr}} = (6.4\sqrt{2}/4)^{-1} = 0.44$. I am grateful to Dr Á. Viúdez for supplying the numerical information reproduced in this footnote.

8. Concluding remarks

All spontaneous imbalance scenarios must involve a radiation reaction of one kind or another. Lighthill's achievement was to find a set of cases in which the effective source strengths are insensitive to the radiation reactions they provoke, with all the conceptual and computational simplifications that follow. By contrast, the non-shallow-water dipole examples involve source strengths that become sensitive to radiation reactions as Rossby numbers R approach unity.

There is yet another intriguing twist. A recent theoretical discovery, the hyperbalance equations, has given us the first fully consistent PV inversion operators of arbitrarily high formal accuracy. A quick review of

the essentials can be found in McIntyre (2008), and a thorough and comprehensive development of the theory, including mathematical demonstrations that it has to take the generic form it does, can be found in Mohebalhojeh and McIntyre (2007a). Like their predecessors, going back to Hinkelmann's forecast initialization work of the 1950s, these highly accurate inversion operators depend on computing diagnostic estimates of time derivatives $\partial^n/\partial t^n$ of the flow fields. So if a flow is exactly steady, then the time derivatives and their diagnostic estimates should all go to zero and the PV inversion should become exact, just as it does in trivial cases like steady circular vortices. But how does that square with the discovery of the new dipole solutions? Can one "invert" the PV field in such a way as to obtain the comoving gravity waves as well, as recently suggested for quite different reasons by Hakim (2008)?

The answer is probably yes and no. It should be no for diffusionless, ideal-fluid dynamics because it is unlikely that any inversion operator would make mathematical sense for a steady but singular flow field. Such a flow field would be expected from the nature of the wave capture process and the finite-amplitude validity, albeit dynamical instability, of plane inertia–gravity waves. Such a flow field would also violate the diffusionless "sign reversal property" discussed in Ford et al. (2000). The answer should be yes when the inversion operators are generalized to include nonideal flow with, for instance, artificial diffusivities or hyperdiffusivities such as those used in numerical models. In that case one expects to find ranges of small diffusivities and Rossby numbers R for which the departure from exact steadiness is exponentially small in R—the captured gravity waves having exponentially small amplitudes and the dipole's decay being correspondingly slow—and for which a high-order PV inversion operator has an exponentially small error and, in particular, delivers a close approximation to the complete flow field including the diffusively damped gravity waves approaching capture.

One further point seems worth making. The need to replace the slow manifold by the fuzzy "slow quasimanifold," whatever its thinness (section 4), seems to be a generic and deeply important insight, originally coming out of the cases studied by Lighthill, Errico, Warn, and others but now, it seems, having still wider relevance. For one thing, a generically fuzzy or chaotic structure is strongly indicated by dynamical systems theory, beginning with the standard example of the homoclinic neighborhood in perturbed simple pendulum problems, with the pendulum moving slowly near its unstable equilibrium in partial analogy to the vortical motion in the fluid problem. And in the fluid problem the chaotic

structure is no more than one naturally expects from the Lighthill picture together with the conspicuous unsteadiness, and the apparently chaotic evolution, of most cases of vortical motion. It is natural to expect at least this level of insight to apply to continuous stratification as well as to shallow water.

However, the new dipole examples—even more clearly than the quasi-steady frontal examples of Snyder et al. (1993)—have revealed an important variation on the generic theme, because they show that in stratified flows the spontaneous emission of gravity waves can be a steady process somewhat like mountain wave generation. If nothing else happens, the waves undergo capture and never escape from their "prison" within the dipole. But such idealized scenarios are overwhelmingly improbable in practice, important though they have turned out to be for broadening our theoretical insight.

Imagine, then, a pair of dipoles in collision, or a dipole interacting with almost any other vortex structure in its surroundings. It would not take much vortex-flow unsteadiness to allow some of the gravity waves to escape from their prison within each dipole and thereafter to become part of the ambient field of freely propagating gravity waves, much as in OSD95 and its successor studies. All these gravity waves can be regarded as contributing to the fuzziness of the slow quasimanifold.

So now there comes yet another new insight: that the slow quasimanifold owes its thinness not only 1) to the Lighthill mechanism for large-scale gravity waves and 2) to jet flaccidity or fluviality in Gulf-stream-like cases with meander scales $\gg L_D$, but also 3) to the generic vulnerability of small-scale gravity waves to wave capture. For such waves, escape from the prison of a progenitor vortex dipole is unlikely to result in prolonged freedom. Because of the tendency toward passive-tracer behavior, there will be a robust statistical bias toward subsequent wave capture. Such a bias is clear from random-straining models such as that of Haynes and Anglade (1997). It now seems that this, too, must be part of why atmospheric and oceanic flows often stay close to balance, and that it should count as a distinct third mechanism contributing thereto.

recent insights into the mathematical issues, which in diffusive versions of these problems involve the extremely smooth behavior known as Gevrey regularity.

REFERENCES

Badulin, S. I., and V. I. Shrira, 1993: On the irreversibility of internal-wave dynamics due to wave trapping by mean flow inhomogeneities. Part 1. Local analysis. *J. Fluid Mech.,* **251,** 21–53.

Batchelor, G. K., 1967: *An Introduction to Fluid Dynamics.* University Press, Cambridge, 615 pp.

Billant, P., and J.-M. Chomaz, 2000: Three-dimensional stability of a vertical columnar vortex pair in a stratified fluid. *J. Fluid Mech.,* **419,** 65–91.

Bühler, O., and M. E. McIntyre, 2005: Wave capture and wave–vortex duality. *J. Fluid Mech.,* **534,** 67–95.

Dritschel, D. G., and M. de la Torre Juárez, 1996: The instability and breakdown of tall columnar vortices in a quasi-geostrophic fluid. *J. Fluid Mech.,* **328,** 129–160.

Errico, R. M., 1982: Normal mode initialization and the generation of gravity waves by quasigeostrophic forcing. *J. Atmos. Sci.,* **39,** 573–586.

Ford, R., 1994: The instability of an axisymmetric vortex with monotonic potential vorticity in rotating shallow water. *J. Fluid Mech.,* **280,** 303–334.

——, M. E. McIntyre, and W. A. Norton, 2000: Balance and the slow quasimanifold: Some explicit results. *J. Atmos. Sci.,* **57,** 1236–1254.

——, ——, and ——, 2002: Reply. *J. Atmos. Sci.,* **59,** 2878–2882.

Hakim, G. J., 2008: A probabilistic theory for balance dynamics. *J. Atmos. Sci.,* **65,** 2949–2960.

Haynes, P. H., and J. Anglade, 1997: The vertical-scale cascade of atmospheric tracers due to large-scale differential advection. *J. Atmos. Sci.,* **54,** 1121–1136.

Hoskins, B. J., 1975: The geostrophic momentum approximation and the semi-geostrophic equations. *J. Atmos. Sci.,* **32,** 233–242.

Jones, W. L., 1969: Ray tracing for internal gravity waves. *J. Geophys. Res.,* **74,** 2028–2033.

Koch, S. E., and P. B. Dorian, 1988: A mesoscale gravity wave event observed during CCOPE. Part III: Wave environment and probable source mechanisms. *Mon. Wea. Rev.,* **116,** 2570–2592.

Lighthill, M. J., 1952: On sound generated aerodynamically. I. General theory. *Proc. Roy. Soc. London,* **211A,** 564–587.

——, 1963: Boundary layer theory. *Laminar Boundary Layers,* L. Rosenhead, Ed., Oxford University Press, 46–113.

McIntyre, M. E., 1997: Lucidity and science. I: Writing skills and the pattern perception hypothesis. *Interdiscip. Sci. Rev.,* **22,** 199–216.

——, 2001: Rupert Ford (obituary). *Quart. J. Roy. Meteor. Soc.,* **127,** 1489–1490.

——, 2003: Potential vorticity. *Encyclopedia of Atmospheric Sciences,* Vol. 2, J. R. Holton, J. A. Pyle, and J. A. Curry, Eds., Elsevier, 685–694. [Available online at www.atm.damtp.cam.ac.uk/people/mem/papers/ENCYC/.]

——, 2008: Potential-vorticity inversion and the wave-turbulence jigsaw: Some recent clarifications. *Adv. Geosci.,* **15,** 47–56.

——, and W. A. Norton, 1990: Dissipative wave-mean interactions and the transport of vorticity or potential vorticity. *J. Fluid Mech.,* **212,** 403–435; Corrigendum, **220,** 693.

——, and ——, 2000: Potential vorticity inversion on a hemisphere. *J. Atmos. Sci.,* **57,** 1214–1235; Corrigendum, **58,** 949.

Methven, J., E. Heifetz, B. J. Hoskins, and C. H. Bishop, 2005: The counter-propagating Rossby-wave perspective on baroclinic instability. Part III: Primitive-equation disturbances on the sphere. *Quart. J. Roy. Meteor. Soc.,* **131,** 1393–1424.

Miles, J. W., 1957: On the generation of surface waves by shear flows. *J. Fluid Mech.,* **3,** 185–204.

Miyazaki, T., and Y. Fukumoto, 1992: Three-dimensional instability of strained vortices in a stably stratified fluid. *Phys. Fluids,* **A4,** 2515–2522.

Mohebalhojeh, A. R., and M. E. McIntyre, 2007a: Local mass conservation and velocity splitting in PV-based balanced models. Part I: The hyperbalance equations. *J. Atmos. Sci.,* **64,** 1782–1793.

——, and ——, 2007b: Local mass conservation and velocity splitting in PV-based balanced models. Part II: Numerical results. *J. Atmos. Sci.,* **64,** 1794–1810.

Norton, W. A., 1988: Balance and potential vorticity inversion in atmospheric dynamics. Ph.D. thesis, University of Cambridge, 167 pp.

Nycander, J., D. G. Dritschel, and G. G. Sutyrin, 1993: The dynamics of long frontal waves in the shallow water equations. *Phys. Fluids,* **5,** 1089–1091.

Ólafsdóttir, E. I., A. B. Olde Daalhuis, and J. Vanneste, 2008: Inertia–gravity-wave radiation by a sheared vortex. *J. Fluid Mech.,* **596,** 169–189.

O'Sullivan, D., and T. J. Dunkerton, 1995: Generation of inertia–gravity waves in a simulated life cycle of baroclinic instability. *J. Atmos. Sci.,* **52,** 3695–3716.

Plougonven, R., and C. Snyder, 2005: Gravity waves excited by jets: Propagation versus generation. *Geophys. Res. Lett.,* **32,** L18802, doi:10.1029/2005GL023730.

Rossby, C.-G., 1936: Dynamics of steady ocean currents in the light of experimental fluid mechanics. *Pap. Phys. Oceanogr. Meteor.,* **5,** 1–43.

——, 1940: Planetary flow patterns in the atmosphere. *Quart. J. Roy. Meteor. Soc.,* **66** (Suppl.), 68–87.

Snyder, C., W. C. Skamarock, and R. Rotunno, 1993: Frontal dynamics near and following frontal collapse. *J. Atmos. Sci.,* **50,** 3194–3212.

——, D. J. Muraki, R. Plougonven, and F. Zhang, 2007: Inertia-gravity waves generated within a dipole vortex. *J. Atmos. Sci.,* **64,** 4417–4431.

Taylor, G. I., 1931: Effect of variation in density on the stability of superposed streams of fluid. *Proc. Roy. Soc. London,* **132A,** 499–523.

Temam, R., and D. Wirosoetisno, 2007: Exponential approximations for the primitive equations of the ocean. *Discrete Contin. Dyn. Syst.,* **7B,** 425–440.

Thorncroft, C. D., B. J. Hoskins, and M. E. McIntyre, 1993: Two paradigms of baroclinic-wave life-cycle behaviour. *Quart. J. Roy. Meteor. Soc.,* **119,** 17–55.

Vanneste, J., and I. Yavneh, 2004: Exponentially small inertia–gravity waves and the breakdown of quasigeostrophic balance. *J. Atmos. Sci.,* **61,** 211–223.

Van Tuyl, A. H., and J. A. Young, 1982: Numerical simulation of nonlinear jet streak adjustment. *Mon. Wea. Rev.,* **110,** 2038–2054.

Viúdez, Á., 2001: The relation between Beltrami's material vorticity and Rossby–Ertel's potential vorticity. *J. Atmos. Sci.,* **58,** 2509–2517.

——, 2006: Spiral patterns of inertia–gravity waves in geophysical flows. *J. Fluid Mech.,* **562,** 73–82.

——, 2007: The origin of the stationary frontal wave packet spontaneously generated in rotating stratified vortex dipoles. *J. Fluid Mech.,* **593,** 359–383.

——, 2008: The stationary frontal wave packet spontaneously generated in mesoscale dipoles. *J. Phys. Oceanogr.,* **38,** 243–256.

——, and D. G. Dritschel, 2004: Optimal potential vorticity balance of geophysical flows. *J. Fluid Mech.,* **521,** 343–352.

Warn, T., 1997: Nonlinear balance and quasi-geostrophic sets. *Atmos.–Ocean,* **35,** 135–145.

Wirosoetisno, D., 2004: Exponentially accurate balance dynamics. *Adv. Diff. Equations,* **9,** 177–196.

Zülicke, C., and D. Peters, 2006: Simulation of inertia–gravity waves in a poleward-breaking Rossby wave. *J. Atmos. Sci.,* **63,** 3253–3276.

——, and ——, 2008: Parameterization of strong stratospheric inertia–gravity waves forced by poleward-breaking Rossby waves. *Mon. Wea. Rev.,* **136,** 98–119.